Dynamics of conformation changes in full-length Phytochrome from cyanobacterium *Synechocystis* sp. PCC6803 (Cph1) monitored by time-resolved translational diffusion detection

Kimitoshi Takeda and Masahide Terazima*

Department of Chemistry, Graduate School of Science, Kyoto University, Kyoto 606-8502, Japan

* Corresponding author:

mterazima@kuchem.kyoto-u.ac.jp, phone/fax number +81-75-753-4026

Abstract

Phytochromes (Phys) are photoreceptor proteins that sense red/far-red light in plants, fungi, and bacteria. The proteins consist of a light-sensing photosensory module and a signaling output module, which is typically a histidine kinase (HK) domain in bacteriophytochromes. Although the time-resolved detection of the HK domain is essential to obtain insights into the reaction mechanism of photoactivation, it has been very difficult to detect the change. Here, the reaction of Cph1, one of the Phys found in the cyanobacterium *Synechocystis* sp. PCC6803, was studied using time-resolved translational diffusion detection. It was found that the kinetics of the HK domain movement of Cph1 dimer can be monitored successfully. The diffusion coefficient of the Cph1 dimer decreases significantly with a time constant similar to that of the final step of the reaction monitored by the transient absorption method (780 ms), whereas the monomer does not exhibit this change. We attribute this change to the close-to-open type of conformational change in the HK domain of the Cph1 dimer without the secondary structure change. The similar rate with that from the transient absorption method suggests that the proton uptake at His260 is the rate-determining step of the conformation change.

Phytochromes (Phys) are red/far-red light-sensor proteins in higher plants, fungi, and bacteria.[1,2] Phys are converted between the thermodynamically stable red light-absorbing (Pr) state and the far-red light-absorbing (Pfr) state depending on the light condition. Cph1 is one of the Phys found in cyanobacterium *Synechocystis* sp. PCC6803.[3] The primary structure of Cph1 consists of the N-terminal photosensory module (PSM) and the C-terminal histidine kinase (HK) domain as an output module. The PSM contains three domain structures: PAS (Period/ARNT/Single-minded), GAF (cGMP phosphodiesterase/adenylyl cyclase/FhlA), and PHY (phytochrome-associated) domains. A chromophore is the open-chain tetrapyrrole phycocyanobilin (PCB), which is covalently bound to the cysteine residue (C259) in the GAF domain. Cph1 is considered to be a light-dependent sensory HK.[3,4] The Pr and Pfr states were phosphorylated and dephosphorylated states, respectively.[3,4] The reaction and the conformation changes of Cph1 have been attracting much attention for a long time in attempts to understand the molecular mechanism of the light regulation of the kinase activity. Thus, the photoreaction has been studied by a variety of methods, such as UV-vis absorption spectroscopy,[5–9] FTIR spectroscopy,[10,11] resonance Raman spectroscopy,[9,12,13] circular dichroism (CD) method,[14,15] fluorescence resonance energy transfer detection,[16] analytical ultracentrifugation method,[17] and nuclear magnetic resonance spectroscopy.[18–21]

To reveal the mechanism of the reaction, time-resolved studies are important and the reaction dynamics has been elucidated mostly by the transient absorption (TrA) method.[5–9] These studies showed that the Z to E isomerization around the C15=C16 bond of PCB in the Pr→Pfr reaction takes place with a rate of ~60 ps and an intermediate (Lumi-R) is created. Some intermediates are then formed over microseconds to several seconds and the Pfr state is finally created. However, the absorption detection method struggles to detect conformation changes except in the environment around the chromophore. It is important and essential to detect the dynamics of the conformation change in the HK domain to understand the mechanism of the kinase activity; however, it is not apparent whether a TrA signal contains any information of possible changes in the HK domain, because it is located rather far from the chromophore. The CD spectrum, which is sensitive to the secondary structure, did not exhibit any change in the HK domain.[14] This result indicates that the conformation change in the HK domain is not a change in the secondary structure. Since the dimer form is known to be essential for the HK reaction,[22–25] the kinase activity might be regulated by modulating the distance between the HK domains of the dimer form. Limited proteolysis[26] and site-directed spin

labelling and pulsed electron–electron double resonance spectroscopy (SDSL-PELDOR) showed that the neighboring PHY domains in the PSMs became close and the relative distance between the PHY and the catalytic adenosine triphosphate(ATP)-binding (CA) domains within the same monomer unit was increased.[6] However, the reaction kinetics in the changes of the HK domain are still unclear, such as when does the conformation change in the HK domain occur? A difficulty in solving this problem is that there is no appropriate detection method to trace the possible conformation change in the HK domain, if it exists.

We investigated the photoreaction dynamics of Cph1 using the transient grating (TG) method. The TG method has been reported as being powerful for detecting spectrally silent dynamics in the time domain.[27–41] We previously investigated the photoreaction dynamics of Cph1Δ2, which lacks the HK domain of Cph1.[27] The diffusion coefficient was found to change with a time constant of 400 μs during the Pr→Pfr conversion; this change was attributed to a change in the orientation (quaternary structure) of the dimer. Furthermore, the measurements of some mutants clearly show that this dimer reorientation was triggered by a conformational change in the tongue region. In this study, we applied the TG technique to identify the reaction dynamics of full-length Cph1. We successfully detected the conformation change kinetics of the HK domain. As far as we know, this is the first report of dynamical detection of the HK domain movement. On the basis of obtained results, we discuss the conformational changes and dynamics of Cph1.

Materials and Methods

Expression and Purification

For producing a protein construct with a C-terminal His_6 tag , a DNA fragment encoding Cph1 (residues M1-N748) was cloned into the pQE70 vector(Qiagen, Venlo, The Netherlands). The chromophore (PCB) was induced by plasmid pKT271.[27,42] *Escherichia coli* strain JM109 was cotransformed with the Cph1 and pKT271 plasmids. The expression condition of Cph1 was similar to that of Cph1Δ2.[27] In this case of full length Cph1, NaCl was not used for the Tris buffer to avoid oligomerization. The proteins were extracted by a French pressure cell. The extracted protein was purified by HisTrap HP affinity column (GE Healthcare, Chicago, IL, USA).[27] The protein was further purified using a HiPrep 26/60 S-300 High Resolution (GE Healthcare) size exclusion chromatography (SEC) column with the Tris buffer. Aggregated

proteins were mainly removed in this process. After that, the proteins were incubated overnight in the Pr state at 4 °C in slightly acidic phosphate buffer (6.4 mM NaH_2PO_4, 13.6 mM Na_2HPO_4, 20% [v/v] glycerol, and 1 mM DTT [pH = 6.8]). For further purification to remove higher oligomers and apo-proteins, the sample was injected in a SEC column (Superdex 200 Increase 10/300 GL column; GE Healthcare), which was equilibrated in the Tris buffer containing 150 mM NaCl, and 1mM DTT at 4 °C. The apo-protein was removed at this step to improve the specific absorbance ratio (SAR) value. As described above, Cph1 tends to form oligomers in the presence of NaCl with a rather high concentration; therefore, the samples were immediately diluted 20 times with the Tris buffer without NaCl to prevent the formation of the oligomers. Finally, Cph1 was dissolved in the Tris buffer containing 50 mM NaCl and 1 mM DTT. The SAR value of Cph1 in this study was about 0.8–0.9. Previous research reported that the SAR value of holo-Cph1 is about 1.0; therefore, our sample contained approximately 80–90% holo-protein. The Cph1 concentration was calculated using the extinction coefficient of the Pr state (86 $mM^{-1}cm^{-1}$ at 660 nm).

Cph1Δ2 (residues M1-E514) was prepared in the same way as reported previously.[27] Cph1Δ2 at pH = 7.8 was dissolved in the same buffer as that for Cph1. Cph1Δ2 at pH = 6.5 was dissolved in the phosphate buffer (6.4 mM NaH_2PO_4, 13.6 mM Na_2HPO_4,50 mM NaCl, 5% (v/v) glycerol, and 1 mM DTT).

Preparation of Pr and red light-irradiated states

The Pr and red light-irradiated (RL) states were respectively prepared by illumination with 720 ± 10 nm and 660 ± 10 nm continuous light.[27] In the RL state, the Pfr/Pr ratio was about 70/30.

TrA measurement

The experimental setup for TrA measurement was similar to that reported previously.[27] A laser pulse (615 nm) from a YAG laser pumped-dye laser was used for the photoexcitation of the sample in a 2 mm path length cell. The absorption change was detected by using a probe light at 720 ± 10 nm from the Xe lamp. The sample solution was irradiated by 785 nm light before every shot of the excitation pulse to recover the sample to the Pr state completely. All measurements were carried out at room temperature (23 °C).

CD measurements

CD spectra were recorded by a method reported before.[27] In this study, the measurements were carried out in the Tris buffer containing 50 mM NaCl and 1 mM DTT and the concentration of the sample was 2.5 μM. The CD spectra were averaged 30 times.

SEC measurements

The ÄKTA purifier system with Superdex 200 Increase 10/300 GL column (GE Healthcare) equilibrated with the Tris buffer containing 150 mM NaCl and 1 mM DTT was used for the SEC measurements. The SEC measurements were carried out at room temperature (23 °C). For the size markers, a gel filtration standard (Bio-Rad, Hercules, CA, USA) was used .[27] The detection wavelength was 660 nm for the Pr state. The concentrations of the eluted solutions were determined from the absorbance at the elution peak using the extinction coefficient of the Pr state.

TG measurement

The TG measurement was performed by a similar setup to that reported previously.[27] The same excitation pulse light as that for the TrA experiment was used. For probing the created grating, continuous wave light at 785 nm from a diode laser was introduced into the grating region. Before every shot of the photoexcitation pulse, the sample solution was irradiated by continuous light at 720 nm to convert back the created Pfr to Pr. The light intensity of the probe light was set to be weak enough (<10 mW) for avoiding the conversion from Pfr to Pr by the probe light.It was confirmed that the probe light did not affect the reaction dynamics by measuring the signal at different probe light intensities.

The signals were detected by the photomultiplier tube and averaged about 30 times by a digital oscilloscope. The grating wavenumber (q) was calculated from the decay rate of the thermal grating signal of a calorimetric reference solution.[27] All measurements were carried out at room temperature (23 °C).

Results

Absorption detection

Before reporting the TG measurements, we first describe the reaction kinetics monitored by the light absorption method. The absorption spectra of Cph1 in the Pr and the red light-irradiated (RL) states are shown in Fig. 1 (A) and (B). The spectra of Cph1Δ2 measured under

the same conditions are also shown for comparison. These spectra resemble each other, which indicates the negligible influence of the HK domain in the absorption spectrum. Fig. 1(C) shows the temporal profile of the absorption changes $I_{TrA}(t)$ of Cph1 and Cph1Δ2 after photoexcitation at 50 μM probed at 720 nm. The qualitative features of both signals are similar. We analyzed $I_{TrA}(t)$ using a sum of exponential functions:

$$I_{TrA}(t) = \beta\left[\sum_{i=1}^{n} A_i \exp(-t/\tau_i) + C\right] \quad (1)$$

where β and C are constants, A_i and τ_i are the amplitude and the time constant of intermediate *i*, respectively. The time profiles of both signals within this experimental time window (60 μs-10 s) are fitted well by a sum of four exponential functions. The time constants τ_1–τ_4 for the best fit of Cph1 signal are 260 μs, 1.3 ms, 33 ms, and 780 ms. These time constants are similar to those reported previously (300 μs, 3.0 ms, 22 ms, 500 ms).[6] The best-fit parameters including the amplitudes are listed in Table 1. The time constants for Cph1Δ2 are 260 μs, 4.6 ms, 46 ms, and 1.0 s. These results clearly show that the influence of the HK domain monitored by the absorption method is minor and it is not clear how information on the HK kinetics can be extracted from these signals.

(A)

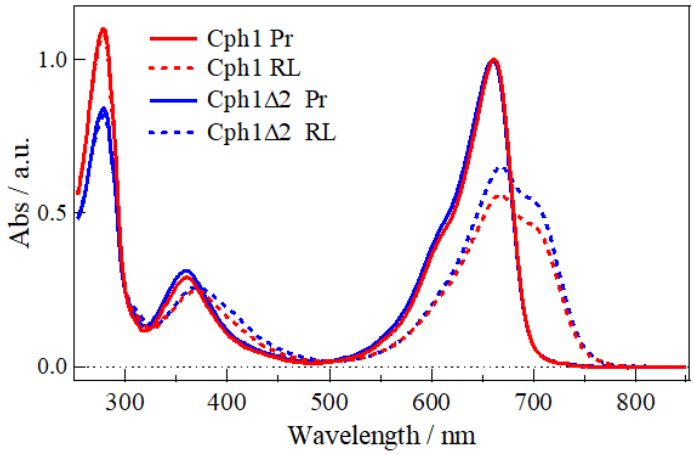

(B)

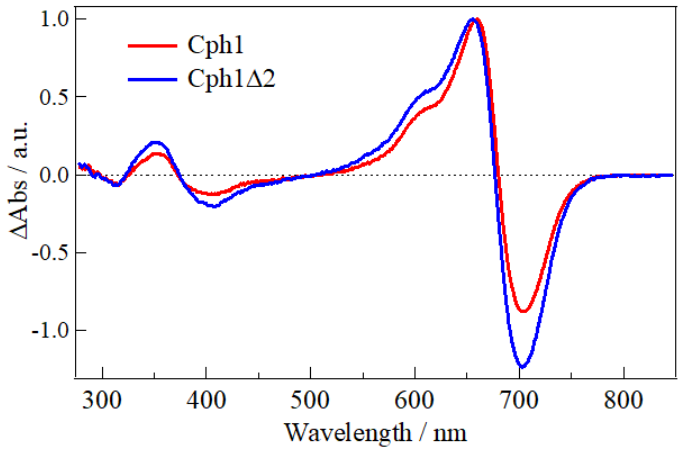

(C)

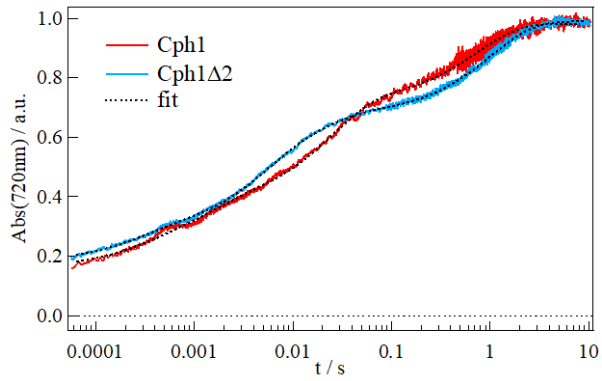

Figure 1. (A) UV-vis absorption spectra of Cph1 (red) and Cph1Δ (blue). The solid lines and dashed lines represent Pr and RL states, respectively. The spectra of each samples were normalized to the peak intensity of the Q_y band in the Pr state. (B) The difference absorption spectra of Cph1 (red) and Cph1Δ2 (blue). The spectra were normalized at the peak of the Pr state. (C) Time traces of the absorption change of Cph1 (red) and Cph1Δ2 (blue) at 50 μM probed at 720 nm. The fitted curves with eq.1 is shown by dotted black lines.

Table 1 Time constants (τ_i) and relative amplitudes (A_i) determined by the fitting of the TrA signal of Cph1 and Cph1Δ2

	τ_1 (A_1)	τ_2 (A_2)	τ_3 (A_3)	τ_4 (A_4)
Cph1	260 μs (9%)	1.3 ms (18%)	33 ms (41%)	780 ms (32%)
Cph1Δ2	260 μs (13%)	4.6 ms (30%)	46 ms (19%)	1.0 s (38%)

Secondary structure and oligomeric states

To examine the secondary structure content and the oligomeric state of Cph1, the CD and SEC measurements were performed. The CD spectra of Cph1 in the Pr and RL states are shown in Fig. 2(A). Although a slight decrease in the CD intensity was observed for the RL state, both spectra are very similar. Since the difference in the CD spectra (Pr - RL) of Cph1 and Cph1Δ2[27] are similar within the experimental uncertainty (Fig.S1), the observed slight CD change may be attributed to the secondary structural change in the "tongue region", of which conformation change has been reported for Cph1Δ2.[27] Since the size of the tongue region (P442-Q490) is very small compared with the full length Cph1 (M1-N748), the weak change in the CD spectrum due to this region is reasonable.

(A)

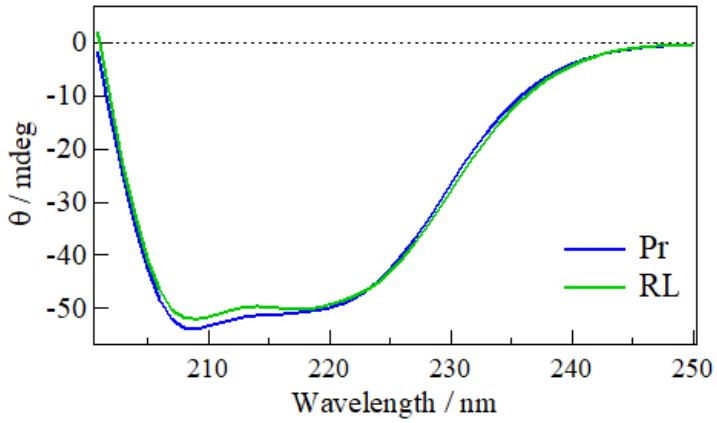

(B)

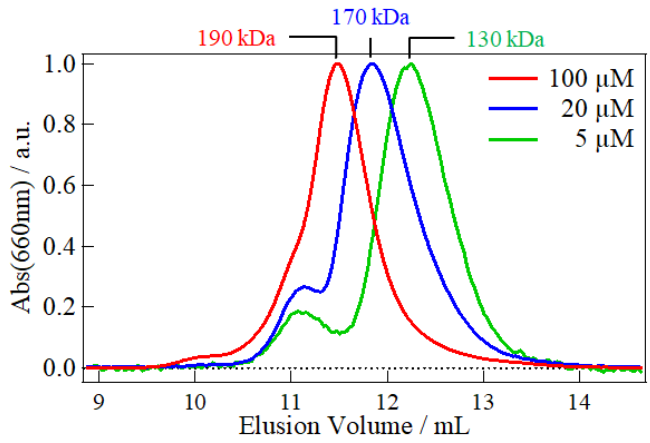

Figure 2. (A) CD spectra of Cph1 in the Pr (blue) and RL (green) states. (B) SEC elution profile of Cph1 in Pr state detected at 660 nm. The initial concentrations of the sample are listed in the legend.

Figure 2(B) shows the elution profiles of Cph1 in the Pr state at several concentrations. The profiles are normalized by the peak intensity. Two peaks were observed at the low concentration (5 μM for injection). The apparent molecular masses of the major and minor bands correspond to 130 kDa and 230 kDa, respectively. The theoretical molecular mass of the Cph1 monomer is 85 kDa, and the apparent masses of the monomer and the dimer measured by the SEC method were reported previously as 110 kDa and 210 kDa, respectively.[22] According to these data, the major and minor bands of Fig. 2(B) are assigned to the monomer and dimer, respectively.

With increasing concentrations, the peak position of the major band shifts to a larger molecular mass. At the injection concentrations of 20 μM and 100 μM, the molecular masses of the major bands were 170 kDa, and 190 kDa, respectively. We consider that this peak shift is due to the dynamical equilibrium between the monomer and the dimer during the elution. Therefore, the apparent molecular mass of this band should be an average mass weighted by the relative population. We roughly estimated the dissociation constant K_D from this apparent molecular mass. Assuming that 130 kDa and 230 kDa are apparent molecular masses of the monomer and the dimer, the relative fraction ratio of the monomer to the dimer at the injection of 20 μM (170 kDa band) is calculated to be 60/40 (monomer/dimer). Moreover, the concentration of the eluted solution at this injection of 20 μM was determined to be 1.3 μM using the absorbance of the main peak and extinction coefficient of the Pr state (86 $mM^{-1}cm^{-1}$ at 660 nm). From these data, K_D of Pr is estimated to be 1.2 μM. Previously, K_D of Cph1 in a buffer (50 mM Tris, 5mM EDTA, pH7.8) at 15 °C was estimated to be 5 ± 3 μM using the fluorescence resonance energy transfer method.[16] Thus, the above interpretation of the peak shift is reasonable because these values were not very different.

Other than the concentration-dependent major band, it is interesting to observe the minor band at the apparent molecular mass of the dimer. The peak position of this minor peak was almost independent of the concentration and the relative intensity became higher with increased concentrations. This band is separated from the major band; therefore, the equilibrium between

the monomer and the dimer is slow enough not to be averaged during the elusion process. These observations suggest that two types of the dimer may exist in the Pr state.

Conformation change detected by diffusion

The TG method was used to investigate the reaction dynamics of Cph1. The sample solution is photoexcited by an interference pattern of the excitation light and the light-induced refractive index change is detected by the diffraction of another probe beam in the time domain. The principle of the TG measurement has been described in more detail previously.[27–41] Since the dimer form is important for the photoreaction of Cph1, we focused on the TG signal of the dimer. Fig. 3(A) shows a typical TG signal of Cph1 at 20 μM, $q^2 = 3.6 \times 10^{10}$ m^{-2}, and sufficiently strong excitation light intensity (>300 μJ/mm^2). According to K_D in the above section, Cph1 at this concentration exists mostly in the dimer form and the signal dominantly comes from the dimer. This observation was confirmed by the concentration-dependent experiment and is described later. Furthermore, the excitation light intensity is strong enough to saturate the light absorption of the dimer to produce the RL state. The light-intensity dependence of the TG signal is shown in Supporting Information, Fig. S2.

(A)

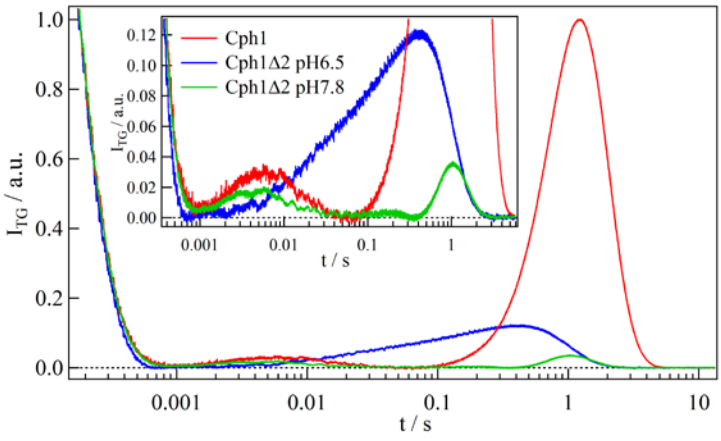

(B)

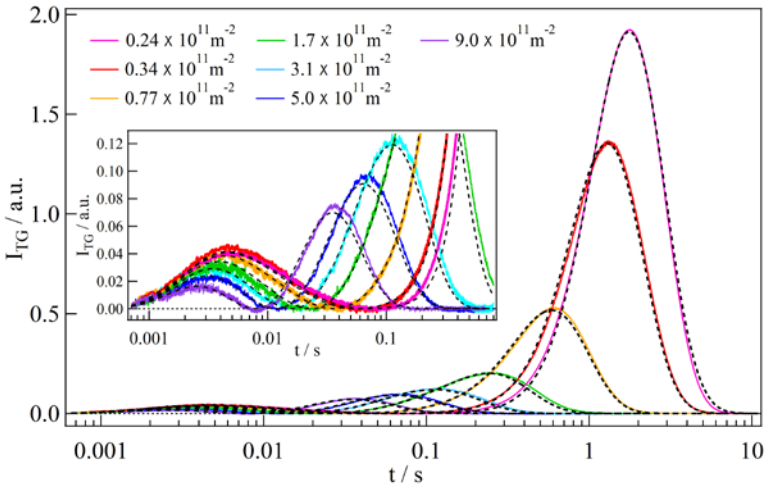

Figure 3. (A) Typical TG signals of Cph1 (red) and Cph1Δ2 (pH = 6.5, blue, and pH = 7.8, green) measured under the same conditions (20 μM and a q^2 of 3.6×10^{10} m^{-2} probed at 785nm). The signals are magnified and shown in the inset. (B) The q^2 dependence of the TG signal of Cph1 at a concentration of 20 μM. The signals in a short time region are magnified and shown in the inset. The q^2 values are listed in the legend. The best-fit curves are shown by the broken lines.

Table 2 Relative refractive index changes (δn) and diffusion coefficients ($D/10^{-11}m^2$ s^{-1}) determined from the TG signal after photoexcitation of the full-length Cph1

	Pr	I_1	I_2	I_3	Pfr
δn	1.0 (fixed)	1.0042	0.9877	0.9979	0.9699
D	4.2 (fixed)			4.0	2.8

The observed TG signal initially rose with the time response of our system (~10 ns), it decayed until ~100 μs and two rise–decay components appeared (Fig. 3(A)). Since the rate constant of the initial decay component agrees with $D_{th}q^2$ (D_{th}: thermal diffusivity) under this condition, this decay component is assigned to the thermal grating signal. The signal after the thermal grating should be the species grating components, which represent transformation of

chemical species and the diffusion processes. Thus, the time profile should be expressed by an equation:

$$I_{TG}(t) = \alpha\{\delta n_{th}\exp(-D_{th}q^2t) + \delta n_{spe}(t)\}^2 \quad (2)$$

where α is a constant representing the system sensitivity, δn_{th} is the pre-exponential factor of the thermal grating component, and $\delta n_{spe}(t)$ represents the species grating component. It has been shown that the time profile of the species grating component reflects chemical reaction kinetics and diffusion processes.[27–41] Since the first rise-decay profile of the signal is rather insensitive to q^2 as shown in Fig. 3(B), this component mostly determined by the reaction kinetics. On the other hand, the rise-decay profile in the last part of the signal significantly depends on q^2 indicating that it represents the protein diffusion (diffusion signal). We first qualitatively explain the diffusion signal.

As described before,[27] if a reaction completes and the diffusion coefficient does not change in the observation time window, the profile of the species grating signal may be expressed by:

$$\delta n_{spe}(t) = -\delta n_{Pr}\exp(-D_{Pr}q^2t) + \delta n_{Pfr}\exp(-D_{Pfr}q^2t) \quad (3)$$

where $\delta n_{Pr}(>0)$ and $\delta n_{Pfr}(>0)$ are the initial refractive index changes due to the reactant and the product, respectively. D_{Pr} and D_{Pfr} are the diffusion coefficients of the reactant (Pr) and the product (Pfr), respectively. The TG signal of this component generally exhibits a rise-decay profile (diffusion signal) and the intensity of this diffusion signal depends on the difference in the diffusion coefficients between the reactant and product as well as the magnitudes of the refractive index change.

We found that the changes in the refractive index for the rise and decay components of the diffusion signal are negative and positive, respectively. From the signs and eq. (3), we identified that the rise and decay components represent, respectively, the diffusion of the reactant (Pr) and the intermediates in this time range or the final product (Pfr). Since the rate of the rise component was faster than that of the decay, it is apparent that the diffusion coefficient decreases during the Pr→Pfr reaction of Cph1.

For comparison, the TG signal of Cph1Δ2 was measured under the same conditions (Fig. 3(A)). Interestingly, although the reactions monitored by the light-absorption detection method of Cph1Δ2 are very similar to that of Cph1, the TG signals are very different. In particular, the amplitude of the diffusion signal is significantly enhanced for Cph1. The equation describing the diffusion signal (eq. (3)) shows that the intensity of the diffusion signal depends on the

difference between D_{Pr} and D_{Pfr}. Qualitatively, the intensity is larger as the difference increases. Therefore, the stronger diffusion signal for Cph1 indicates that the diffusion change is larger for Cph1 compared with that for Cph1Δ2, which lacks the HK domain. This observation indicates that the large diffusion change in Cph1 came from the changes in the HK domain. This is a very interesting and important result, because detection of movement in the HK domain has been very difficult. Indeed, despite the extensive studies on Cph1 to date, the dynamics of the HK domain have not been reported. However, it is now possible to use the diffusion coefficient to monitor the kinetics of the HK movement.

Fig. 3(B) shows the TG signals of Cph1 at various q^2 at 20 μM. For this measurement, we used the enough strong light intensity (>300 μJ/mm^2) to saturate the excitation. To compare the diffusion signal intensity measured at different q^2, the signals were normalized with the intensity of the species grating, in which the diffusion and thermal contributions were negligible. By this way, the q^2 dependence of the TG signal normalized by the concentration of photoreacted species was determined. The diffusion signal increased gradually with increased observation time, i.e., decreasing q^2 (Fig. 3(B)). Since the diffusion signal intensity increases with an increase in the difference of the diffusion coefficients, the dramatic increase in intensity after ~300 ms clearly shows that structural change in the protein occurs during this time period.

We then quantitatively analyzed the q^2-dependent signals. Considering the q^2-dependence of the diffusion signal and the reaction dynamics probed by the TrA method, we attempted to fit the signal based on scheme I:

$$\mathrm{Pr} \xrightarrow{h\nu} \mathrm{I_1} \xrightarrow{k1} \mathrm{I_2} \xrightarrow{k2} \mathrm{I_3} \xrightarrow{k3} \mathrm{Pfr} \qquad \text{(Scheme I)}$$

where k_1–k_3 denote the reaction rate constants. Moreover, I_1–I_3 represent the intermediate species of this reaction. The I_1 intermediate is the first intermediate created after our system response time. An analytical equation for fitting the TG signal is given in Supporting Information SI-3. Since there are many parameters in the equation, ambiguities in the adjustable parameters by the signal fitting cannot be avoided without any restriction. For reducing ambiguity of the fitting, we estimated D_{Pr} using the SOMO (SOlution MOdeller) program with the crystal structure of the full-length phytochrome-activated diguanylyl cyclases from *Idiomarina* sp. (*Is*PadC) (PDB: 5LLX, $D_{Pr} = 4.2 \times 10^{-11}$ m^2/s).[43,44] Even using this restriction, the signal can be fitted reasonably well by a rather wide range of the time constants $k_1^{-1} - k_3^{-1}$ of 1.2±0.1 ms, 50±20 ms, and 700±100 ms. It is interesting to note that the time

constants from the TrA signal (1.3 ms, 33 ms, and 780 ms) are within this range. Of course, the rates of the diffusion change are not necessary to be the same as the rates from the TrA signal. However, the similarity of the rates determined from the TrA detection and diffusion detection suggests that these time constants could be the same. Here, for reducing the ambiguity of the fitting, we assume the adjustable parameters, $k_1^{-1} - k_3^{-1}$ to be 1.3 ms, 33 ms, and 780 ms, respectively, which were obtained from the TrA analysis. We discuss this point later, and show that this assumption is reasonable. Using these restrictions, the adjustable parameters for the fitting (eqs. S-1 and S-2) are the diffusion coefficients for these species (D_i, where i = I_1, I_2, I_3, and Pfr) and the refractive index changes (δn_i, where i = Pr, I_1, I_2, I_3, and Pfr). All TG signals were globally fitted with the same D_i and δn_i. The signals were well reproduced using eqs. S-1 and S-2, and the diffusion coefficients were determined to be $D_{I1} = 4.2 \times 10^{-11}$ m^2/s, $D_{I2} = D_{I3} = 4.0 \pm 0.1 \times 10^{-11}$ m^2/s, and $D_{Pfr} = 2.8 \pm 0.1 \times 10^{-11}$ m^2/s. The other parameters are listed in Table 2. The origin of the diffusion change is discussed in the next section.

It should be noted that the diffusion coefficient change mostly occurs with the time constants of k_1^{-1} and k_3^{-1}. Interestingly, even though the HK domain is located far from the chromophore, the rates of the motion of the HK domain are similar to those of the absorption change in the chromophore. This observation indicates that the conformational change in the HK domain is strongly coupled with the chromophore environment. This coupling is discussed in a later section.

Concentration dependence

The TG signal at various concentrations were measured and shown in Fig. 4(A), which is normalized by the intensity of the species grating signal in a 2–4 ms time range; i.e., the concentration of the photoexcited species. The intensity of the diffusion signal became weaker with decreasing the concentration of Cph1. This concentration dependence is related to the origin of the diffusion change. Decreases in the diffusion coefficients in many photosensor proteins have been reported to date and are explained in terms of oligomer formations and/or conformation changes of the proteins.[27–41] In the case of Cph1, we excluded the possibility of oligomer formation based on the following two reasons. First, if the decrease in the diffusion coefficient is due to the oligomer formation of the photoexcited species, the decrease in the diffusion signal intensity with decreased concentrations should be explained in terms of the decrease in the oligomer-formation rate. We tried to reproduce the observed concentration-

dependent diffusion signal by adjusting the rate constant of k_3 of Scheme I. However, the signals cannot be fitted consistently by eq. S-2 with a concentration-dependent reaction rate (k_3). Second, although the monomer and dimer forms are well known for Cph1, there has been no indication of the tetramer formation from the photoexcited dimer of Cph1. Therefore, the observed diffusion coefficient change must be due to the conformation change after the transformation from Pr to Pfr.

Based on the above assignment, the observed concentration dependence was attributed to the different reactions of the dimer and monomer, the fraction of which depends on the concentration. This explanation is reasonable, because previous studies showed different higher structural changes between the monomer and dimer. For example, the proteolysis study demonstrated that the light-dependent conformation change in the monomer is minor.[26]

(A)

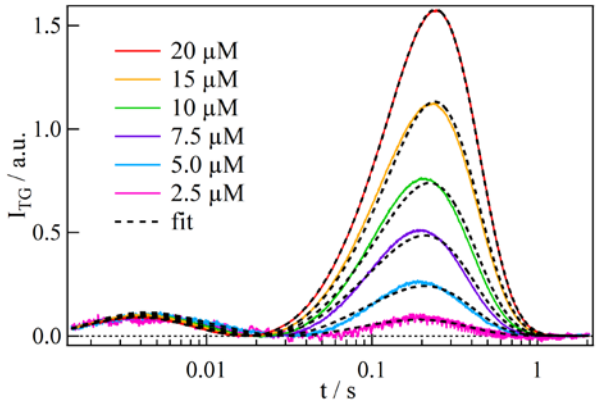

(B)

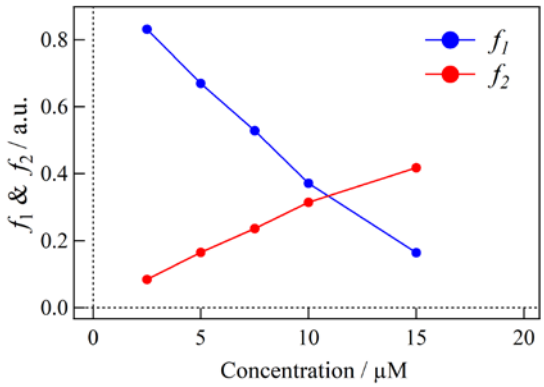

(C)

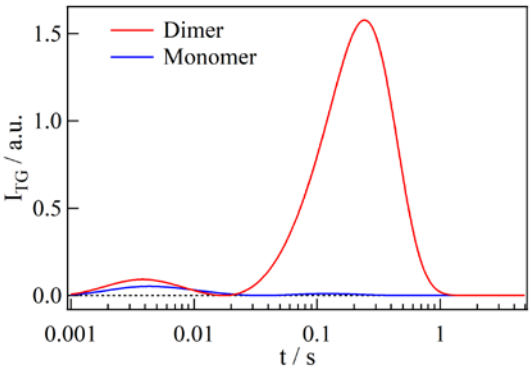

Figure 4. (A) Concentration dependence of the TG signal of Cph1 at a q^2 of 1.8×10^{11} m^{-2}. The concentrations are listed in the legend. The broken lines are the best fitted curves calculated by eq. (4). (B) The relative concentrations of monomer (f_1) and dimer (f_2) are plotted against the total protein concentration (C). (C) The decomposed TG signals of the monomer (blue) and dimer (red) at 20 μM.

The concentration dependence of the diffusion signal was analyzed by using the sum of the reactions of the dimer and the monomer. By expressing the time dependence of the species grating component of the monomer and the dimer as $\delta n_{spe}^{M}(t)$ and $\delta n_{spe}^{D}(t)$, the observed diffusion signals may be expressed by:

$$\delta n_{spe}(t) = f_1 \delta n_{spe}^{M}(t) + 2 f_2 \delta n_{spe}^{D}(t) \qquad (4)$$

where f_1 and f_2 are the relative fractions of the monomer and dimer, respectively; i.e., they are given by f_1=[M]/C and f_2=[D]/C, where C, [M] and [D] are the total protein, monomer, and dimer concentrations, respectively. The total protein concentration was measured using the absorbance of the solution. The factor 2 on the right-hand side of eq. (4) represents two chromophores in the dimer. To simplify the analysis in this study, we assumed that the reaction rates of the absorption change and the refractive index changes in the monomer are the same as those in the dimer. Moreover, our SEC experiment found that dimeric Cph1 was dominant in 9 μM (corresponding to the injection concentration of 100μM (Fig. 2(B))). Therefore, we initially assumed that the TG signal at 20 μM is almost the same as the dimer signal.

Since the diffusion signal became weaker with decreasing the concentrations, we first tried to analyze the molecular diffusion signals using eq. S-2, assuming no diffusion coefficient

change for the monomeric Cph1. The diffusion coefficient of the monomer (5.3×10^{-11} m^2/s) was calculated from D_{Pr} of the dimer (4.2×10^{-11} m^2/s) using the Stokes–Einstein relationship. However, the signal could not be reproduced. Next, we assumed that the diffusion coefficient was very slightly changed at the first step (formation of I_1). Under this assumption, the observed concentration-dependent signals were reproduced well as shown in Fig. 4(A) with adjustable parameters of f_1, f_2, and the diffusion coefficient of the intermediate and the product of the monomer ($5.2 \pm 0.1 \times 10^{-11}$ m^2/s). In Fig. 4(B), f_1 and f_2 are plotted against C, and the determined TG signals of the dimer and the monomer at 20 μM are shown in Fig. 4(C). The TG signal of the monomer is apparently negligibly weak compared with that of the dimer, which confirms that the large diffusion changes dominantly originated from the reaction of the dimer. This result also indicates that the conformation change in the monomer is small and consistent with the previous study using the limited proteolysis.[26]

Discussion

Although the crystal structure of PSM of Cph1 (Cph1Δ2) has been reported previously (PDB: 2VEA, 3ZQ5),[45,46] the structure of the full-length Cph1 (including the HK domain) is not yet known. However, since the sequence homology of the HK domain of Cph1 is very high compared with other HK proteins,[3] it is reasonable to consider that the C-terminal region of Cph1 is similar to other HK domains. Generally, the HK domains consist of two domain structures; the dimerization and histidine phosphotransfer (DHp) domain and the CA domain.[23–25] The DHp domain is composed of two helical structures, which typically form a stable parallel homodimer through a four-helix bundle and the catalytic histidine (His538 in Cph1) exists at the DHp domain. Therefore, it is highly probable that Cph1 forms a parallel dimer through the HK domain. Indeed, the previous study using the SDSL-PELDOR method suggests a parallel dimer form for Cph1.[6] Here, we discuss the conformational dynamics of Cph1 based on the parallel dimer model.

First, we consider the minor diffusion coefficient change with the time constant of 1.3 ms. Previously, we studied the reaction of Cph1Δ2 by the TG method and found that the diffusion coefficient changes with a time constant of 400 μs, 10 ms, and 40 ms.[27] In particular, the major change in the diffusion coefficient occurs with the time constant of 400 μs. Although many studies of Phys suggested the secondary structural change in the ‘tongue region,’[47–54] which is located in the PHY domain and highly conserved over the whole phytochrome

superfamily, we found that the conformation change of the tongue region is not a cause of the major diffusion change.[27] Furthermore, since this change was observed only for the dimer of Cph1Δ2, this change was attributed to the orientation change in the dimer form. The small diffusion coefficient changes in Cph1 with the time constant of 1.3 ms is attributed to the orientation change between two PSMs. Previous SDSL-PELDOR measurements showed that the distance between neighboring PHY domains became shorter by the reaction from Pr to Pfr.[6] Thus, we consider that the small diffusion coefficient changes in Cph1 on this short time scale reflects the interaction change in the neighboring PHY domains of the dimer.

Here, we compare the difference in the diffusion change in PSM between Cph1 and Cph1Δ2. For this purpose, we used the equation $\Delta f = k_B T(1/D_{I2} - 1/D_{Pr})$, where k_B is the Boltzmann constant and T is the temperature, to calculated the increase in friction (Δf) for the translational diffusion in the initial step (D_{Pr}/D_{I2} =1.04) . The increase in friction for Cph1 calculated by this equation is 4.4×10^{-12} kg/s. On the other hand, the increase in friction by the orientation change in the dimer structure of Cph1Δ2 is 4.9×10^{-11} kg/s, which is much larger than that of Cph1.[27] There are two possibilities to explain this difference.

A possible origin could be the different orientations of PSM between Cph1 and Cph1Δ2. In our previous study, the photoreaction dynamics of Cph1Δ2 were studied in a buffer solution at pH = 6.5, and this pH is the same as the crystallization pH of Cph1Δ2, which forms the antiparallel dimer.[45,46] Therefore, Δf of Cph1Δ2 may be due to the orientation change in the antiparallel dimer structure. However, since Cph1 most possibly forms the parallel dimer as stated above, the smaller Δf caused by the PSM change may reflect the orientation change in the parallel dimer. In any cases, it is clear that the conformation change in Cph1 until a few hundreds milliseconds is minor.

Another possible cause of the smaller change may be the restriction effect by the presence of the HK domain. Since the HK domain is relatively large, the presence of the HK domain with PSM may hinder the movement of PSM. Furthermore, since the DHp domain in the HK domain is considered to be the dimerization site, it is highly probable that this dimerization effect restricts the orientation movement of PSM.

We next consider the major diffusion change during the 780 ms process, which is attributed to the conformation change in the two HK domains. Although there have been numerous researches on Phys, molecular details of the conformation change in the HK domain has been still unclear. It has been proposed that the dimer interface is broken in the Pfr state

from the small-angle X-ray scattering (SAXS) measurements of the bacteriophytochrome from *Deinococcus radiodurans* (DrBphP).[55] A recent single-particle electron microscopy study on DrBphP reported that there are two kinds of arrangements of the HK domain in the Pfr state.[56] One is that the two HK domains are in contact (closed), and the other is the two HK domains separated (open). This close-open scheme is consistent with the crystal structures and SAXS measurement of the PSM fragments.[47,50,55,57] On the other hand, the time-resolved SAXS data of DrBphP suggests a rotation motion of the CA domain.[58] It is difficult to determine which model is appropriate for Cph1. However, according to the Stokes–Einstein relationship and the Perrin equation, the diffusion coefficient is known to be rather insensitive to small shape changes in macromolecules.[59] Thus, we consider that the observed large change in the diffusion coefficient is an indication of a significant conformation change in the HK domain, such as to induce a significant increase in the hydration area of the HK domain. Furthermore, it is shown here that this change occurs only for the dimer of Cph1. Therefore, we consider that the closed-to-open structural change in the CA domain is plausible for the Pr to Pfr reaction of Cph1, even though the dimer interface of the DHp domain could be intact.

This model (closed-to-open structural change in the CA domain maintaining the secondary structure) is consistent with the observed small change in the CD spectrum. Furthermore, this model is also consistent with the mechanism of the autophosphorylation of the HK domains proposed so far.[23–25] In many cases, the HKs exist as the dimer and the CA domains are activated by changing the binding site of the catalytic histidine residue, and this change is induced by the tertiary structural change in the DHp domain. In Cph1, since the Pr and Pfr states are, respectively, autophosphorylated (active) and dephosphorylated (inactive) states, it is reasonable to consider that the CA domain dissociates from the DHp domain to be open during the Pr→Pfr reaction.

In this study, we found that this significant structural change in the HK domain takes place in the final step of the Pr→Pfr reaction monitored by the TG and TrA method. Initially, we thought that the HK domain could be controlled by the orientation change in PSM, which contains the chromophore. However, the conformation change in PSM occurs in a much faster time region (1.3 ms). Therefore, it is apparent that the HK domain movement is governed by another factor. We explain this difference in terms of the proton uptake and the secondary structural change in the tongue region as follows. The tongue region forms the β-sheet structure in the Pr state and converts to the α-helix in the Pfr state. This change leads to the alteration of

the tongue region length and may result in orientation change in the dimer of PSM.[53] Furthermore, using resonance Raman scattering and Fourier transform infrared measurements of the bathy bacteriophytochrome from *Agrobacterium tumefaciens* (Agp2), it was reported that conformation change in the tongue region is governed by the proton translocation in the vicinity of the chromophore;[49] i.e., the proton uptake by highly conserved His278 (His260 in Cph1) residue near the chromophore induces the α-helix formation of the tongue region. Based on these findings, we consider that a trigger reaction that induces the conformation change in the HK domain occurs by a scheme of:

proton uptake → α-helix formation of the tongue region

→ conformation change in the HK domain.

These processes may be very fast. In the case of Cph1, the TrA method with a pH indicator dye was used to study the proton release and uptake processes.[8] The proton uptake was found to occur in the final step of the Pr→Pfr reaction. Thus, the same rate of the proton uptake as that of the HK domain movement determined in this research supports the above signal transduction scheme and suggests that the proton-uptake process is the rate-determining step.

Furthermore, this signal transduction scheme suggests that the rate of the HK domain movement detected by the diffusion detection can be the same as that detected by the chromophore absorption change. Since the HK domain is located far from the chromophore-binding site, the global change in the HK domain can be spectrally silent. However, it has been reported that an important residue for the proton uptake is a His residue, which is highly conserved in every Phys and located near the chromophore. For example, the TrA measurement of the prototypical bacteriophytochrome from *Agrobacterium tumefaciens* (Agp1) showed that the light-induced proton uptake from the solvent is accompanied by the protonation change in His250 residue.[60] A similar role of His260 in Cph1 was reported using site-directed mutagenesis.[61] These data strongly indicate that His260 plays a crucial role for the proton-uptake phase. Since this residue locates near the chromophore, the protonation change, hence the dislocation of the HK domain, is detectable by the absorption detection method. This consideration supports that the assumption used in the analysis of the TG signal is appropriate.

The time-resolved SAXS measurements showed that the major structural change in DrBphP occurs during the second-to-last step of the absorption change (2.6 ms). This time constant is two orders of magnitude shorter than that observed in this study. It is interesting to note that not only the time scale of the HK domain movement, but also the kinetics of

absorption changes are different between DrBphP and Cph1. There are three intermediates (Lumi-R, Meta-Ra, and Meta-Rc) for DrBphP, whereas four intermediates were reported for Cph1. Moreover, the light-induced conformation change in PSM is different. In the Pr→Pfr reaction, while the distance between the neighboring PHY domains becomes shorter for Cph1,[6] the two PHY domains are separated in DrBphP.[56] These reports strongly indicate that the light-induced conformational changes are different between Cph1 and DrBphP, although the structures of the PSM domains are similar each other.[53] The conformation changes of Phys could possess diversity depending on the proteins, even though the structures are similar. The reactions of various Phys should be elucidated in more detail.

In summary, we demonstrated that the translational diffusion coefficient is a useful physical quantity to detect the conformation change in the HK domain of full-length Cph1. A significant change in the diffusion coefficient was observed for the Cph1 dimer, but not for the Cph1 monomer, which indicates that the conformation change in the HK domain to increase the friction for translational diffusion of the monomer is minor. The cause of the diffusion change is attributed to the conformation change in the HK domain, such as the closed-to-open type, which should enhance the hydration. The rate of the conformation change was successfully determined to be 780 ms, which is the final step of the reaction kinetics monitored by the TrA method. Since this final step of the reaction is attributed to the protonation process of His260 of Cph1, we consider that the proton uptake induces the α-helix formation of the tongue region and this change is associated with the conformation change in the HK domain. We consider that the light-induced conformational changes are different between Cph1 and DrBphP suggesting diversity of the conformation changes of Phys depending on the proteins.

SUPPORTING INFORMATION

The difference CD spectra of Cph1 and Cph1Δ2 (SI-1), the laser power dependence of the TG signal (SI-2), and fitting equation of the TG signal (SI-3).

ACKNOWLEDGEMENTS:

The authors are indebted to Prof. T.Kohchi (Kyoto University) for kindly provided the plasmid of Cph1. This work was supported by a Grant-in-aid for Scientific Research (Nos. JP20107003, JP25102004, 25288005, 17H03008)) from MEXT/JSPS (to M.T.).

Accession Code

Cph1:Q55168

Note added in proof. Shortly before a notice of final acceptance of this manuscript on the scientific points, a study using time-resolved SAXS method was reported.[62] The conclusion from SAXS study is consistent with the results and discussion of this study.

REFERENCES

(1) Rockwell, N. C., Su, Y.-S., and Lagarias, J. C. (2006) Phytochrome Structure and Signaling Mechanisms. *Annu. Rev. Plant Biol. 57*, 837–858.

(2) Ulijasz, A. T., and Vierstra, R. D. (2011) Phytochrome structure and photochemistry: Recent advances toward a complete molecular picture. *Curr. Opin. Plant Biol. 14*, 498–506.

(3) Yeh, K. C.,Wu. S. H., Murphy, J. T., and Lagarias, J. C. (1997) A Cyanobacterial Phytochrome Two-Component Light Sensory System. *Science. 277*, 1505–1508.

(4) Psakis, G., Mailliet, J., Lang, C., Teufel, L., Essen, L. O., and Hughes, J. (2011) Signaling kinetics of cyanobacterial phytochrome Cph1, a light regulated histidine kinase. *Biochemistry 50*, 6178–6188.

(5) Kirpich, J. S., Mix, L. T., Martin, S. S., Rockwell, N. C., Lagarias, J. C., and Larsen, D. S. (2018) Protonation Heterogeneity Modulates the Ultrafast Photocycle Initiation Dynamics of Phytochrome Cph1. *J. Phys. Chem. Lett. 9*, 3454–3462.

(6) Heyes, D. J., Khara, B., Sakuma, M., Hardman, S. J., O'Cualain, R., Rigby, S. E., and Scrutton, N. S. (2012) Ultrafast Red Light Activation of Synechocystis Phytochrome Cph1 Triggers Major Structural Change to Form the Pfr Signalling-Competent State. *PLoS One 7*, e52418

(7) Heyne, K., Herbst, J., Stehlik, D., Esteban, B., Lamparter, T., Hughes, J., and Diller, R. (2002) Ultrafast dynamics of phytochrome from the cyanobacterium Synechocystis, reconstituted with phycocyanobilin and phycoerythrobilin. *Biophys. J. 82*, 1004–1016.

(8) van Thor, J. J., Borucki, B., Crielaard, W., Otto, H., Lamparter, T., Hughes, J., Hellingwerf, K. J., and Heyn, M. P. (2001) Light-induced proton release and proton uptake reactions in the cyanobacterial phytochrome Cph1. *Biochemistry 40*, 11460–11471.

(9) Remberg, A., Lindner, I., Lamparter, T., Hughes, J., Kneip, C., Hildebrandt, P., Braslavsky, S. E., Gärtner, W., and Schaffner, K. (1997) Raman spectroscopic and light-induced kinetic characterization of a recombinant phytochrome of the cyanobacterium Synechocystis. *Biochemistry 36*, 13389–13395.

(10) Foerstendorf, H., Lamparter, T., Hughes, J., Gärtner, W., and Siebert, F. (2000) The photoreactions of recombinant phytochrome from the cyanobacterium Synechocystis: a low-temperature UV-Vis and FT-IR spectroscopic study. *Photochem. Photobiol. 71*, 655–661.

(11) van Thor, J. J., Fisher, N., and Rich, P. R. (2005) Assignments of the Pfr - Pr FTIR difference spectrum of cyanobacterial phytochrome Cph1 using15N and13C isotopically

labeled phycocyanobilin chromophore. *J. Phys. Chem. B 109*, 20597–20604.
(12) Velazquez Escobar, F., Lang, C., Takiden, A., Schneider, C., Balke, J., Hughes, J., Alexiev, U., Hildebrandt, P., and Mroginski, M. A. (2017) Protonation-dependent structural heterogeneity in the chromophore binding site of cyanobacterial phytochrome Cph1. *J. Phys. Chem. B 121*, 47–57.
(13) Mroginski, M. A., von Stetten, D., Escobar, F. V., Strauss, H. M., Kaminski, S., Scheerer, P., Günther, M., Murgida, D. H., Schmieder, P., Bongards, C., Gärtner, W., Mailliet, J., Hughes, J., Essen, L. O., and Hildebrandt, P. (2009) Chromophore structure of cyanobacterial phytochrome Cph1 in the Pr state: Reconciling structural and spectroscopic data by QM/MM calculations. *Biophys. J. 96*, 4153–4163.
(14) Park, C. M., Shim, J. Y., Yang, S. S., Yang, J. G., Kim, J. I., Luka, Z., and Song, P. S. (2000) Chromophore-apoprotein interactions in Synechocystis sp. PCC6803 phytochrome Cph1. *Biochemistry 39*, 6349–6356.
(15) Rockwell, N. C., Shang, L., Martin, S. S., and Lagarias, J. C. (2009) Distinct classes of red/far-red photochemistry within the phytochrome superfamily. *Proc. Natl. Acad. Sci. 106*, 6123–6127.
(16) Otto, H., Lamparter, T., Borucki, B., Hughes, J., and Heyn, M. P. (2003) Dimerization and inter-chromophore distance of Cph1 phytochrome from Synechocystis, as monitored by fluorescence homo and hetero energy transfer. *Biochemistry 42*, 5885–5895.
(17) Strauss, H. M., Schmieder, P., and Hughes, J. (2005) Light-dependent dimerisation in the N-terminal sensory module of cyanobacterial phytochrome 1. *FEBS Lett. 579*, 3970–3974.
(18) Rohmer, T., Strauss, H., Hughes, J., de Groot, H., Gärtner, W., Schmieder, P., and Matysik, J. (2006) 15N MAS NMR studies of Cph1 phytochrome: Chromophore dynamics and intramolecular signal transduction. *J. Phys. Chem. B 110*, 20580–20585.
(19) Strauss, H. M., Hughes, J., and Schmieder, P. (2005) Heteronuclear solution-state NMR studies of the chromophore in cyanobacterial phytochrome Cph1. *Biochemistry 44*, 8244–8250.
(20) Song, C., Psakis, G., Lang, C., Mailliet, J., Gartner, W., Hughes, J., and Matysik, J. (2011) Two ground state isoforms and a chromophore D-ring photoflip triggering extensive intramolecular changes in a canonical phytochrome. *Proc. Natl. Acad. Sci. 108*, 3842–3847.
(21) Song, C., Rohmer, T., Tiersch, M., Zaanen, J., Hughes, J., and Matysik, J. (2013) Solid-

state NMR spectroscopy to probe photoactivation in canonical phytochromes. *Photochem. Photobiol. 89*, 259–273.
(22) Lamparter, T., Esteban, B., and Hughes, J. (2001) Phytochrome Cph1 from the cyanobacterium Synechocystis PCC6803 purification, assembly, and quaternary structure. *Eur. J. Biochem. 268*, 4720–4730.
(23) Jacob-Dubuisson, F., Mechaly, A., Betton, J. M., and Antoine, R. (2018) Structural insights into the signalling mechanisms of two-component systems. *Nat. Rev. Microbiol. 16*, 585-593.
(24) Zschiedrich, C. P., Keidel, V., and Szurmant, H. (2016) Molecular Mechanisms of Two-Component Signal Transduction. *J. Mol. Biol. 428*, 3752–3775.
(25) Bhate, M. P., Molnar, K. S., Goulian, M., and Degrado, W. F. (2015) Signal Transduction in Histidine Kinases: Insights from New Structures. *Structure 23*, 981–994.
(26) Esteban, B., Carrascal, M., Abian, J., and Lamparter, T. (2005) Light-induced conformational changes of cyanobacterial phytochrome Cph1 probed by limited proteolysis and autophosphorylation. *Biochemistry 44*, 450–461.
(27) Takeda, K., and Terazima, M. (2018) Photoinduced Orientation Change of the Dimer Structure of the Pr-I State of Cph1Δ2. *Biochemistry 57*, 5058–5071.
(28) Iwata, K., Terazima, M., and Masuhara, H. (2018) Novel physical chemistry approaches in biophysical researches with advanced application of lasers: Detection and manipulation. *Biochim. Biophys. Acta. Gen. Subj. 1862*, 335–357.
(29) Nakasone, Y., Ono, T. A., Ishii, A., Masuda, S., and Terazima, M. (2007) Transient dimerization and conformational change of a BLUF protein: YcgF. *J. Am. Chem. Soc. 129*, 7028–7035.
(30) Nakasone, Y., Eitoku, T., Matsuoka, D., Tokutomi, S., and Terazima, M. (2007) Dynamics of Conformational Changes of Arabidopsis Phototropin 1 LOV2 with the Linker Domain. *J. Mol. Biol. 367*, 432–442.
(31) Terazima, M. (2006) Diffusion coefficients as a monitor of reaction kinetics of biological molecules. *Phys. Chem. Chem. Phys. 8*, 545–557.
(32) Nakasone, Y., Eitoku, T., Matsuoka, D., Tokutomi, S., and Terazima, M. (2006) Kinetic measurement of transient dimerization and dissociation reactions of Arabidopsis phototropin 1 LOV2 domain. *Biophys. J. 91*, 645–653.
(33) Khan, J. S., Imamoto, Y., Yamazaki, Y., Kataoka, M., Tokunaga, F., and Terazima, M.

(2005) A biosensor in the time domain based on the diffusion coefficient measurement: Intermolecular interaction of an intermediate of photoactive yellow protein. *Anal. Chem. 77*, 6625–6629.
(34) Takakado, A., Nakasone, Y., Okajima, K., Tokutomi, S., and Terazima, M. (2017) Light-Induced Conformational Changes of LOV2-Kinase and the Linker Region in Arabidopsis Phototropin2. *J. Phys. Chem. B 121*, 4414–4421.
(35) Takakado, A., Nakasone, Y., and Terazima, M. (2017) Photoinduced dimerization of a photosensory DNA-binding protein EL222 and its LOV domain. *Phys. Chem. Chem. Phys. 19*, 24855–24865.
(36) Choi, S., Nakasone, Y., Hellingwerf, K. J., and Terazima, M. (2016) Photochemical Reactions of the LOV and LOV-Linker Domains of the Blue Light Sensor Protein YtvA. *Biochemistry 55*, 3107–3115.
(37) Takeda, K., Nakasone, Y., Zikihara, K., Tokutomi, S., and Terazima, M. (2013) Dynamics of the amino-terminal and carboxyl-terminal helices of arabidopsis phototropin 1 LOV2 studied by the transient grating. *J. Phys. Chem. B 117*, 15606–15613.
(38) Terazima, M. (2011) Studies of photo-induced protein reactions by spectrally silent reaction dynamics detection methods: Applications to the photoreaction of the LOV2 domain of phototropin from Arabidopsis thaliana. *Biochim. Biophys. Acta - Proteins Proteomics 1814*, 1093–1105.
(39) Terazima, M. (2011) Time-dependent intermolecular interaction during protein reactions. *Phys. Chem. Chem. Phys. 13*, 16928–16940.
(40) Nakasone, Y., Eitoku, T., Zikihara, K., Matsuoka, D., Tokutomi, S., and Terazima, M. (2008) Stability of Dimer and Domain-Domain Interaction of Arabidopsis Phototropin 1 LOV2. *J. Mol. Biol. 383*, 904–913.
(41) Hoshihara, Y., Imamoto, Y., Kataoka, M., Tokunaga, F., and Terazima, M. (2008) Conformational changes in the N-terminal region of photoactive yellow protein: A time-resolved diffusion study. *Biophys. J. 94*, 2187–2193.
(42) Mukougawa, K., Kanamoto, H., Kobayashi, T., Yokota, A., and Kohchi, T. (2006) Metabolic engineering to produce phytochromes with phytochromobilin, phycocyanobilin, or phycoerythrobilin chromophore in Escherichia coli. *FEBS Lett. 580*, 1333–1338.
(43) Brookes, E., Demeler, B., Rosano, C., and Rocco, M. (2010) The implementation of SOMO (SOlution MOdeller) in the UltraScan analytical ultracentrifugation data analysis

suite: Enhanced capabilities allow the reliable hydrodynamic modeling of virtually any kind of biomacromolecule. *Eur. Biophys. J. 39*, 423–435.
(44) Gourinchas, G., Etzl, S., Göbl, C., Vide, U., Madl, T., and Winkler, A. (2017) Long-range allosteric signaling in red light–regulated diguanylyl cyclases. *Sci. Adv. 3*, e1602498.
(45) Essen, L. O., Mailliet, J., and Hughes, J. (2008) The structure of a complete phytochrome sensory module in the Pr ground state. *Proc. Natl. Acad. Sci. 105*, 14709–14714.
(46) Mailliet, J., Psakis, G., Feilke, K., Sineshchekov, V., Essen, L. O., and Hughes, J. (2011) Spectroscopy and a high-resolution crystal structure of Tyr263 mutants of cyanobacterial phytochrome Cph1. *J. Mol. Biol. 413*, 115–127.
(47) Burgie, E. S., Zhang, J., and Vierstra, R. D. (2016) Crystal Structure of Deinococcus Phytochrome in the Photoactivated State Reveals a Cascade of Structural Rearrangements during Photoconversion. *Structure 24*, 448–457.
(48) Yang, X., Stojković, E. A., Ozarowski, W. B., Kuk, J., Davydova, E., and Moffat, K. (2015) Light Signaling Mechanism of Two Tandem Bacteriophytochromes. *Structure 23*, 1179–1189.
(49) Velazquez Escobar, F., Piwowarski, P., Salewski, J., Michael, N., Fernandez Lopez, M., Rupp, A., Qureshi, B. M., Scheerer, P., Bartl, F., Frankenberg-Dinkel, N., Siebert, F., Andrea Mroginski, M., and Hildebrandt, P. (2015) A protonation-coupled feedback mechanism controls the signalling process in bathy phytochromes. *Nat. Chem. 7*, 423–430.
(50) Takala, H., Björling, A., Berntsson, O., Lehtivuori, H., Niebling, S., Hoernke, M., Kosheleva, I., Henning, R., Menzel, A., Ihalainen, J. A., and Westenhoff, S. (2014) Signal amplification and transduction in phytochrome photosensors. *Nature 509*, 245–248.
(51) Burgie, E. S., Bussell, A. N., Walker, J. M., Dubiel, K., and Vierstra, R. D. (2014) Crystal structure of the photosensing module from a red/far-red light-absorbing plant phytochrome. *Proc. Natl. Acad. Sci. 111*, 10179–10184.
(52) Stojković, E. A., Toh, K. C., Alexandre, M. T., Baclayon, M., Moffat, K., and Kennis, J. T. (2014) FTIR spectroscopy revealing light-dependent refolding of the conserved tongue region of bacteriophytochrome. *J. Phys. Chem. Lett. 5*, 2512–2515.
(53) Burgie, E. S., and Vierstra, R. D. (2014) Phytochromes: An Atomic Perspective on Photoactivation and Signaling. *Plant Cell Online 26*, 4568–4583.
(54) Anders, K., Daminelli-Widany, G., Mroginski, M. A., von Stetten, D., and Essen, L. O.

(2013) Structure of the cyanobacterial phytochrome 2 photosensor implies a tryptophan switch for phytochrome signaling. *J. Biol. Chem. 288*, 35714–35725.
(55) Takala, H., Björling, A., Linna, M., Westenhoff, S., and Ihalainen, J. A. (2015) Light-induced changes in the dimerization interface of bacteriophytochromes. *J. Biol. Chem. 290*, 16383–16392.
(56) Burgie, E. S., Wang, T., Bussell, A. N., Walker, J. M., Li, H., and Vierstra, R. D. (2014) Crystallographic and electron microscopic analyses of a bacterial phytochrome reveal local and global rearrangements during photoconversion. *J. Biol. Chem. 289*, 24573–24587.
(57) Björling, A., Berntsson, O., Takala, H., Gallagher, K. D., Patel, H., Gustavsson, E., St. Peter, R., Duong, P., Nugent, A., Zhang, F., Berntsen, P., Appio, R., Rajkovic, I., Lehtivuori, H., Panman, M. R., Hoernke, M., Niebling, S., Harimoorthy, R., Lamparter, T., Stojković, E. A., Ihalainen, J. A., and Westenhoff, S. (2015) Ubiquitous Structural Signaling in Bacterial Phytochromes. *J. Phys. Chem. Lett. 6*, 3379–3383.
(58) Björling, A., Berntsson, O., Lehtivuori, H., Takala, H., Hughes, A. J., Panman, M., Hoernke, M., Niebling, S., Henry, L., Henning, R., Kosheleva, I., Chukharev, V., Tkachenko, N. V., Menzel, A., Newby, G., Khakhulin, D., Wulff, M., Ihalainen, J. A., and Westenhoff, S. (2016) Structural photoactivation of a full-length bacterial phytochrome. *Sci. Adv. 2*, e1600920.
(59) Cussler, E. L. (1984) "Diffusion: Mass Transfer in fluid System", Cambridge University Press.
(60) von Stetten, D., Seibeck, S., Michael, N., Scheerer, P., Mroginski, M. A., Murgida, D. H., Krauss, N., Heyn, M. P., Hildebrandt, P., Borucki, B., and Lamparter, T. (2007) Highly conserved residues Asp-197 and His-250 in Agp1 phytochrome control the proton affinity of the chromophore and Pfr formation. *J. Biol. Chem. 282*, 2116–2123.
(61) Hahn, J., Strauss, H. M., Landgraf, F. T., Gimenèz, H. F., Lochnit, G., Schmieder, P., and Hughes, J. (2006) Probing protein-chromophore interactions in Cph1 phytochrome by mutagenesis. *FEBS J. 273*, 1415–1429.
(62) Heyes, D. J., Hardman, S. J. O., Pedersen, M. N., Woodhouse, J., De, La, Mora, E., Wulff, M., weik, M., Cammarate, E., Scrution, N. S., and Schirò, G. (2019) Light-induced structural changes in a full-length cyanobacterial phytochrome probed by time-resolved X-ray scattering. Commun Biol. 2:1.

For Table of Contents Use Only